ACS APPLIED MATERIALS & INTERFACES

Research Article

www.acsami.org

Silica Hybrid Sol–Gel Materials with Unusually High Concentration of Pt–Organic Molecular Guests: Studies of Luminescence and Nonlinear Absorption of Light

Denis Chateau,[†] Frédéric Chaput,[†] Cesar Lopes,[‡] Mikael Lindgren,[§] Carl Brännlund,[‡] Johan Öhgren,[‡] Nikolay Djourelov,[⊥] Patrick Nedelec,[⊥] Cedric Desroches,[∥] Bertil Eliasson,[#] Tomas Kindahl,[#] Frédéric Lerouge,[†] Chantal Andraud,[†] and Stephane Parola*[,†]

[†]Laboratoire de Chimie, Université de Lyon, Université Claude Bernard Lyon 1, ENS Lyon, CNRS UMR5182, Lyon 69364, France

[‡]Information Systems, Swedish Defence Research Agency (FOI), Linköping SE-581 11, Sweden

[§]Department of Physics, Norwegian University of Science and Technology, Trondheim NO-7491, Norway

[⊥]Institut de Physique Nucléaire, Université de Lyon, Université Claude Bernard Lyon 1, CNRS, Villeurbanne, France

[∥]University of Lyon, France

[#]Department of Chemistry, Umeå University, Umeå SE-901 87, Sweden

Supporting Information

ABSTRACT: The development of new photonic materials is a key step toward improvement of existing optical devices and for the preparation of a new generation of systems. Therefore synthesis of photonic hybrid materials with a thorough understanding and control of the microstructure-to-properties relationships is crucial. In this perspective, a new preparation method based on fast gelation reactions using simple dispersion of dyes without strong covalent bonding between dye and matrix has been developed. This new sol–gel method is demonstrated through synthesis of monolithic siloxane-based hybrid materials highly doped by various platinum(II) acetylide derivatives. Concentrations of the chromophores as high as 400 mM were obtained and resulted in unprecedented optical power limiting (OPL) performance at 532 nm of the surface-polished solids. Static and time-resolved photoluminescence of the prepared hybrid materials were consistent with both OPL data and previous studies of similar Pt(II) compounds in solution. The impacts of the microstructure and the chemical composition of the matrix on the spectroscopic properties, are discussed.

KEYWORDS: *sol–gel, hybrid materials, xerogel, monolith, nonlinear absorption, optical power limiting, platinum*

INTRODUCTION

The preparation of inorganic glasses using low-temperature routes (soft-chemistry) has been described as an interesting alternative to conventional glass manufacturing. It is especially appropriate for the preparation of organic–inorganic hybrid composite materials. The low-temperature preparation routes can give hybrid materials containing a mineral part which coexists with an organic part. They can easily be processed as particles, films, or monoliths. This approach has been known for several decades and there has been an intensive activity in this field for the past 20 years.[1−6] Another benefit of the low-temperature route is that thermally sensitive doping agents, such as functional molecular systems or nanostructures, readily can be incorporated in a glassy matrix, to constitute multifunctional hybrid materials with a variety of properties. The interactions between the matrix and the doping agent are controlled by the nature of the organic parts and their concentrations. Silica is a suitable host matrix since it combines good thermal and mechanical properties. In addition, silica exhibits no absorption in the near-UV to near-IR wavelength range and refractive index, which can be advantageous in many optical applications. For instance, a large variety of materials for optical and optoelectronic applications have been developed by trapping active species into the polymeric network of silica-based gels.[1−3,5−11]

Preparation of guest–host systems can proceed through two principal methods. The first method is based on a simple dispersion of the active species in the matrix without strong interaction between the guest system and the silica backbone.[8,9] In the second method, the guest active units are bonded to the silica network through strong chemical bonds.[4−7,10,11] The main drawback of the first method is that the solubility of the guest (organic or organometallic compounds, or inorganic nanomaterials) is often low in the rather polar SiO_2-based gels and xerogels. This approach is appropriate only for applications where low doping levels are adequate.[8,9] In this context, chemical covalent grafting of the molecular species to the silica backbone can be suitable for greatly increasing the concentrations of the guest molecules up to 0.1–0.5 M. The bonding of the doping agent can be accomplished via trialkoxysilyl groups in the organic molecular framework, which are then hydrolyzed and subsequently co-condensed with the silicon

Received: November 7, 2011
Accepted: January 25, 2012
Published: January 25, 2012

   dx.doi.org/10.1021/am2015537 | ACS Appl. Mater. Interfaces 2012, 4, 2369–2377

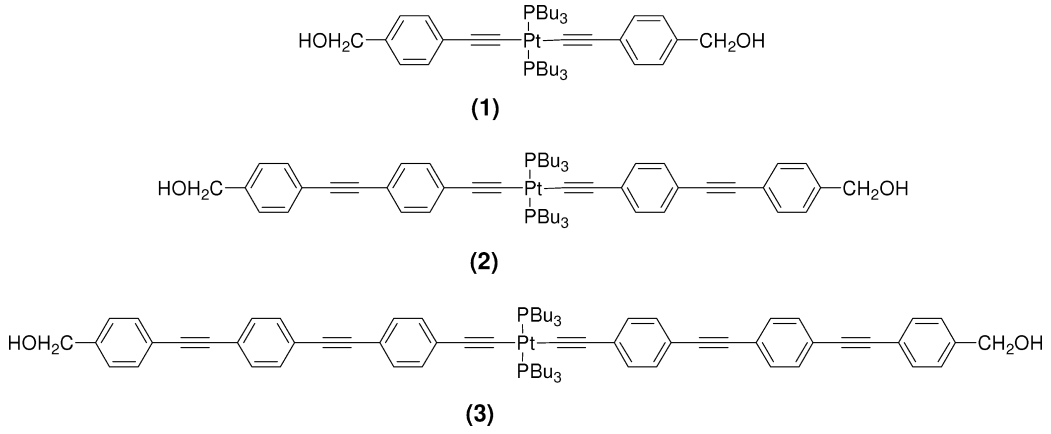

Figure 1. Structures of the chromophores **1**, **2**, and **3**.

alkoxide during the sol–gel process.[10,11] Such a method was previously applied by us for the preparation of glass materials from di(arylethynyl)diphosphine Pt(II) complexes functionalized with siloxane groups on the peripheral aromatic rings.[5,6] Concomitantly, the modification of the matrix precursor by alkyl-substituted alkoxides which confers hydrophobicity to the network, can improve the compatibility between the guest and host. Nevertheless, the grafting may induce structural changes on the functional doping agents and the original properties of the guest chromophores are generally not completely recovered. Moreover, functionalization of the guest chromophore with trialkoxysilyl groups requires multistep synthesis, sometimes complicated and expensive. A limited long-term stability of these functionalized molecules can also be a problem. Further, a high doping ratio in the range 40–50% in weight, which can be required for optical applications, has never been reached using such grafting methodology.

The properties of the hybrids can be strongly influenced by the strengths of the chromophore-matrix interactions, but there are very few reports on detailed investigations of these interactions on the final optical properties.[1−6] Often, the discussions are limited to the compatibility and solubility of grafted systems, compared with dispersed one. Although the question of the relationship between optical properties and interactions in the matrix has been raised, the matter remains underdeveloped.[9]

Another general issue, in both approaches, concerns the control of the drying and densification step which usually is slow and tedious in order to prevent the host matrix from cracking. To overcome such issues, different procedures have been developed. In several of them DCCA (drying control chemical additives) such as formaldehyde are used to control the ultrastructure of the gel–solid and pore phases.[12,13] This method gives a rapid (a few hours instead of tens of days) gelation, aging, drying, and densification of the sol–gel-derived monoliths. However, this implies contamination of the final materials as a result of the presence of the DCCA.

In this work, we report a new procedure, based on the sol–gel technique, that enables the preparation of hybrid monolithic materials with very high concentration of doping agents. The process can also be modified for the preparation of films or powders and can be adapted to both dispersed and grafted systems. The method is here exemplified by the preparation of efficient solid materials for optical power limiting (OPL) applications, where mechanical and thermal properties are combined with high loading of the OPL molecules. Nonlinear absorption materials have the ability to distinct between low- and high-intensity light, where the latter is attenuated. One of the applications for OPL materials is protection of optical sensors against intense (laser) light.[14,15] High-performance optical limiting materials should exhibit broadband high extinction of intense electromagnetic radiation and high transmission for low intensity radiation, and at the same time have high light-induced damage threshold and function in a broad temperature range. Much of the work on nonlinear absorbers has so far been dominated by studies on liquid samples. However, in real applications solid-state materials are preferred. The attention is therefore turning to guest–host solid-state materials. Polymer host systems such as PMMA, silica and gels have been investigated. However, PMMA and related polymers have low T_g, around 100 °C,[16] whereas a silica host has a wide temperature working range. With the introduction of a method to achieve high mass-% doping of different chromophores together with the possibility to cut and polish the materials to different shapes, silica guest–host materials have now emerged as one of the best alternatives for high performance optical limiting materials.[5,6,17−22]

To demonstrate the new sol–gel approach, Pt(II) diacetylide complexes were chosen as OPL chromophores. They have proven to be good candidates for optical power limiting applications through an efficient intersystem crossing and absorption by their relatively long-lived excited triplet state.[23−33] However, acetylide ligands without polar groups tend to give Pt(II) complexes with low solubility in common solvents such as ethers, alcohols and water, but proper substitution on, for instance, ligand aryl rings can result in better solubility. This makes the Pt- acetylides interesting models for fundamental studies of the structure–property relationship in hybrid materials. The new sol–gel approach presented here allows for formation of unique solid-state materials at unusually high concentration of Pt-acetylides, without strong (covalent) bonding between the organic and the silica network, preserving the OPL and photophysical properties of the parent compounds. An investigation of their spectroscopic properties and function, through the OPL capability, is here used to demonstrate the approach in a demanding application.

MATERIALS PREPARATION

One of the drawbacks in the preparation of sol–gel hybrid materials is the possibility to achieve high doping concentration. Here, we describe a new method for the preparation of

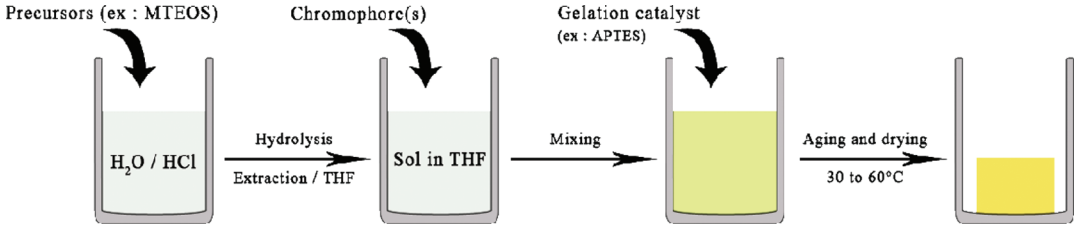

Figure 2. Elaboration of hybrid monoliths. Going from solution (left) to monoliths (right).

sol−gel hybrid materials that incorporates molecular guests at very high concentrations without necessity to covalently graft the dyes to the inorganic network. Three platinum-acetylide based chromophores (**1**−**3**) were used in this work, see structures in Figure 1. These were selected on the basis of results from earlier photophysical studies on platinum complexes in solution.[24,25] The structures of the chromophores are terminated with CH_2OH groups in order to facilitate the comparison of the spectroscopic results with results obtained on similar chromophores in solution and on grafted hybrids and to increase the polarity of the compounds.[6] The optical properties of the chromophores are sensitive to structural changes and molecular interactions, and they are thus interesting sensors for investigations of structural changes in the matrix. For example, it has been shown that the phosphorescence of complexes very similar to **2** is strongly reduced by the presence of oxygen,[25,34] and that formation of singlet oxygen occurs via the phosphorescent triplet state.[35]

The routes for preparation of **1**−**3** are analogous to that in previously published work.[25] The alkynes used as ligands in the Pt(II) complexes were synthesized using Cu/Pd-induced coupling between an alkyne and an aryl halide as originally described by Sonogashira et al.[36] The synthesis is described in the Supporting Information.

An important feature of the current sol−gel method is that the condensation time is shortened, with a rapid fixation of the solid network, which prevents aggregation and crystallization of molecular organic or inorganic guests.[37] During the first step of the process a precursor, methyltriethoxysilane (MTEOS), is hydrolyzed using HCl aqueous solution at pH =3.8. Other precursors, or mixtures of different precursors, can also be used for modification of the matrix structure and tuning of the hydrophilicity. Some examples are glycidoxypropyltriethoxysilane (GLYMO), vinyltriethoxysilane (VTEOS), acetamidopropyltriethoxysilane (AAPTES), propanamidopropyltriethoxysilane (PrAPTES) and benzamidopropyltriethoxysilane (BAPTES). After hydrolysis, water and alcohol are removed under vacuum. The resulting viscous sol is dissolved in diethyl ether to remove water after phase separation. Finally, a solvent exchange is undertaken by addition of tetrahydrofuran (THF) and evaporation of the remaining diethyl ether. The obtained sol is mixed with a solution of the chromophore in THF and placed in a mold. The crucial step corresponds to a fast and efficient condensation of the sol that leads to a highly cross-linked gel. This fast condensation is initiated by a quick addition of a base to the mixture (*i.e.*, aminopropyltriethoxysilane, APTES), see Figure 2, leading to a condensation ratio of the cross-linked gel equal to or greater than 0.7, where 1.0 corresponds to full cross-linking. Thus, the short gelation time associated with a high condensation rate "freezes" the distribution of the doping species and limits their aggregation/crystallization even for extremely highly concentrated sols. Mixtures of doping agents can also easily be achieved with this process, even if they have different solubilities in the sol.

The hybrid materials prepared are homogeneous and can be shaped as porous or dense monoliths, films and powders. The intermolecular interactions of the host agents can easily be tuned by controlling the concentration and the fast condensation, and can be minimized if necessary even at high payloads. Concentrations over 50% in mass can be prepared with a homogeneous dispersion of the doping agent (Figure 3). No other method is known by us for preparation of such high-doped materials.

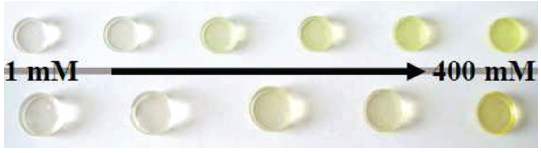

Figure 3. Hybrid materials prepared from MTEOS and chromophore **2** with different chromophore contents (from 1 mM to 400 mM, diameter 15 mm).

Indeed, the process can occur at elevated temperatures in closed vessels allowing dissolution of the doping agent (if the solubility constant increases with increasing temperature), where the instantaneous condensation allows cross-linking of the matrix with a resulting homogeneous dispersion of the doping agent. Following this procedure at normal temperature and pressure, concentrations up to four times higher than obtained in saturated liquids could be reached. After cooling, the dispersion is preserved in the final solid since the doping agent no longer has mobility in the matrix. The crude silica glasses, see Figure 3, can be cut and polished to give high quality optical glasses as shown in Figure 4.

STRUCTURE OF THE MATRIX VERSUS THE CHEMICAL COMPOSITION

The chemical composition of the matrix depends on the initial sol. A mixture of organosilanes can contribute in the modification of the hydrophilicity and microstructure of the final xerogel. Materials from different precursor mixtures using

Figure 4. Cut and polished monolithic hybrid silica glasses of approximately 2.5 cm diameter and a thickness of 1 mm.

dx.doi.org/10.1021/am2015537 | *ACS Appl. Mater. Interfaces* 2012, 4, 2369−2377

MTEOS, GLYMO, VTEOS, AAPTES, PrAPTES, and BAPTES were prepared. Typical materials of different compositions are summarized in Table 1. Solid state NMR and porosity measurements were used to assess their chemical and morphological structure (see below).

Table 1. Sol Compositions and Condensation Ratios

precursors (molar ratio)	$\%T_1$	$\%T_2$	$\%T_3$	condensation ratio of the liquid sol (%)
MTEOS (100%)	4	54	41	78
MTEOS (100%)[a]	<1	32	68	89
VTEOS (100%)[a]	<1	31	69	90
GLYMO/MTEOS (20/80)	7	39	54	82
AAPTES/MTEOS (20/80)	4	37	59	85
BAPTES/MTEOS (20/80)	16	39	45	76

[a]Prepared using 20 g/L aqueous citric acid solution, instead of pH 3.8 (HCl).

Degree of Condensation from NMR Spectroscopy. ^{29}Si NMR was recorded in order to investigate the condensation rates of the sols prior to the final condensation reactions. Integration of the NMR signals gave the relative amounts of the mono-, di- and tricondensed silanes, denoted T1, T2, and T3, respectively. No silanes with remaining alkoxy groups were detected after the quick condensation step, which means that the hydrolysis was finalized. The condensation ratio was determined taking in consideration the number of condensed groups on each precursor using the following formula: condensation ratio = %T3 + 2/3%T2 + 1/3%T1. Depending on the formulation and the hydrolysis conditions the condensation ratio varied between 70 and 92%. Table 1 shows the condensation ratios of different prepared sols.

Porosity Measurements. It is important to note that there is a correlation between the chemical composition of the starting sol and the microstructure of the final monolithic materials. The monoliths show no mesoporosity as determined by BET gas absorption[38] or thermoporosimetry[39] measurements on the monoliths. SEM and TEM were performed but no micropores could be observed. The number and size of the pores did not allow imaging using these techniques. However, investigations using positron annihilation lifetime spectroscopy (PALS) revealed different microstructures. The positron annihilation lifetime spectroscopy is a well-recognized powerful, nondestructive tool for microstructure studies of condensed matter.[40] In many insulators the positron can form a bound state with a host electron, positronium (Ps), which exists in the singlet (parapositronium, p-Ps) or the triplet (orthopositronium, o-Ps) state with lifetimes in vacuum $\tau_{v,p\text{-}Ps} = 0.125$ ns and $\tau_{v,o\text{-}Ps} = 142$ ns. In matter, o-Ps is confined in free volumes (pores) and its lifetime $\tau_{o\text{-}Ps}$, is shortened, because of interaction with pore walls. The shortening of the $\tau_{o\text{-}Ps}$ lifetime is directly correlated to the size of the pores.[41,42] Thus, when Ps formation is detected, valuable information on nano and subnanometer scale porosity can be extracted. The analysis of the PALS spectra (see Figure 5) with up to five discrete exponential components indicated presence of o-Ps with pick-off annihilation lifetime of the order of few nanoseconds and for some of the samples additional long-lived (few tens of nanoseconds) lifetimes. A discussion of the determined short lifetimes, ~0.140 ns due to p-Ps annihilation and ~0.400 ns due to free e^+ annihilation, is beyond the scope of this report. Table 2 summarizes the experimental results on the PALS measurements. The sizes of the pores where Ps are confined were calculated, assuming spherical shape, from the long lifetimes given in Table 2, and from $\tau_{o\text{-}Ps}$ by the help of the extended Tao-Eldrup (ETE) model[43] and Sudarshan model.[44] The latter model is necessary to apply for lifetimes >20 ns due to the measurements in air and expected interconnected pores in the sample.

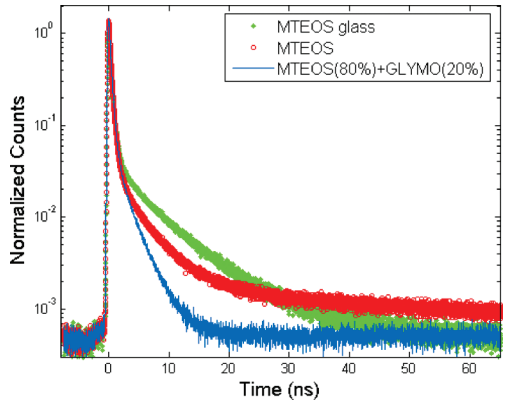

Figure 5. Positron annihilation lifetime spectra.

The result for MTEOS shows the presence of three long lifetimes (τ_3, τ_4, τ_5) suggesting three types of pores. The largest pores have significantly larger pore radii compared to the smallest pores. However, in MTEOS(80%)+GLYMO(20%), the longest-lived component (τ_5) is missing. Although the o-Ps lifetime is successfully used for pore size determination, the o-Ps intensity is influenced not only by the available free volume but also by many other factors such as temperature, free radicals, additives, polar groups in the chemical structure which usually act as Ps inhibitors, etc. This is why in general the o-Ps intensity cannot be used directly as a measure of the relative pore concentration. In the particular case of the present study there are no Ps inhibitors neither in MTEOS or GLYMO. Thus, we can conclude that the lack of the fifth component for MTEOS(80%)+GLYMO(20%) indicate absence of the largest pores seen in MTEOS glasses.

OPTICAL AND LUMINESCENCE PROPERTIES OF THE HYBRID MATERIALS

Materials doped with different mass percentages of compounds **1**, **2**, and **3** were prepared, cut, and polished in order to investigate the optical properties (Figures 3 and 4). The optical transmission spectra for a series of different nominal concentrations (0.1−400 mM) of compound **1**-based sol−gel glasses are shown in Figure 6. As expected, the absorption is red-shifted with increased concentration of the chromophore. In the same plot, the transmission curves for the chromophores **2** and **3** are also shown, at their nominal loading concentrations of 400 and 50 mM, respectively.

The prepared materials showed high linear transmission throughout the whole visible range and have excellent optical quality after cutting and polishing. Thus, in conjunction with a nonlinear absorption property (section further below), the materials are good candidates for solid state OPL applications.

Because of the strong absorption at wavelengths below 400 nm it was not possible to study luminescence of the excited states via the usual transmission excitation. Instead data were

Table 2. Long Lifetimes τ_3, τ_4, τ_5 (ns) and Relative Intensities I_3, I_4, I_5 (%) Due to *o*-Ps Pick-off Annihilation and the Calculated Corresponding Pore Radii (R, nm) via the ETE-Sudarshan Model

sample	I_3 (%)	I_4 (%)	I_5 (%)	τ_3 (ns)	τ_4 (ns)	τ_5 (ns)	R_3 (nm)	R_4 (nm)	R_5 (nm)
MTEOS	7.3(5)	23.2(7)	6.5(8)	1.45(26)	6.3(4)	14.4(8)	0.23	0.53	0.79
MTEOS (80%)+GLYMO(20%)	7.3(6)	12.9(7)		1.27(30)	2.7(2)		0.20	0.34	

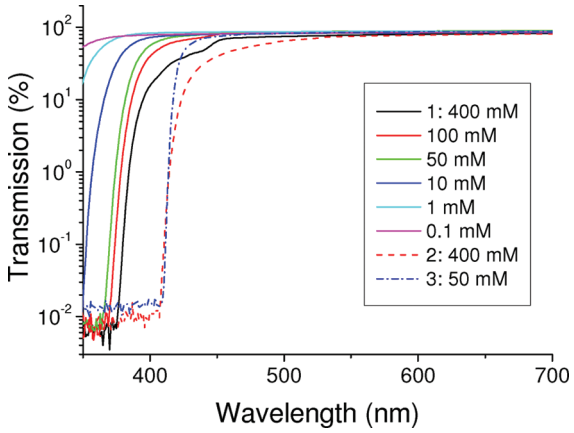

Figure 6. Optical transmission spectra for a series of polished 1 mm thick sol–gel glass materials doped with **1**, **2**, and **3**, respectively. Notice that the vertical scale is logarithmic in order to better compare the low and high levels of transmission.

recorded by inclining the sample and using a grazing angle of incidence of approximately 22° for the excitation light. Time- and spectrally resolved signals could then be recorded at 90° angle from the excitation path. This experimental setup also minimizes reabsorption of the emitted light at the shorter wavelength side of the emission band. A band-pass filter was placed in front of the emission collection system to minimize the level of background noise from scattered excitation light.

Emission spectra for excitation wavelength at 300 nm, for glass samples of chromophore **1**, are shown in Figure 7. At low

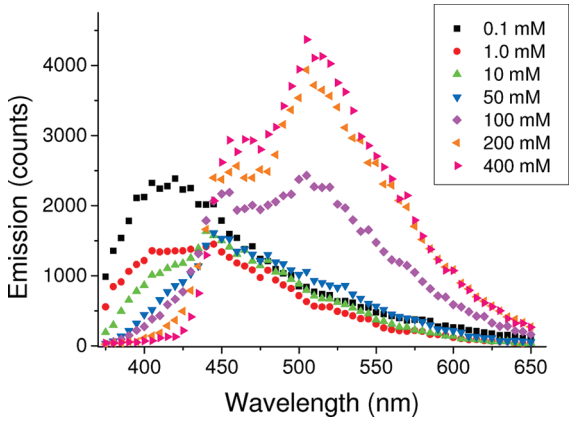

Figure 7. Emission spectra for a series of sol–gels doped with **1** at different concentrations in a MTEOS-based matrix.

concentration there is a dominating contribution from fluorescence (very short decay time; data not shown) at approximately 400–450 nm. However, this is gradually decreased/quenched as the concentration is increased. This is not surprising as already 0.1 mM is considered a high concentration for fluorescence studies in solution.

The calculated average Pt-to-Pt distance between chromophores is for a 1 mM concentration approximately 118 Å. At high concentrations, this results in an efficient quenching via dipolar relaxation mechanisms. Interestingly, the spectral contribution from a broad-band emission at around 525 nm to the total emission increases at chromophore concentrations above 50 mM, which is the well-known phosphorescence of compound **1** and similar structures.[25] This was further verified by performing time-resolved measurements at the emission maximum, with representative data shown in Figure 8. For all

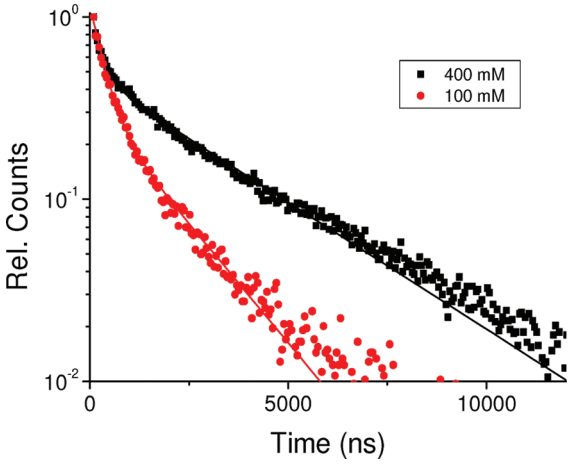

Figure 8. Typical time-resolved emission for two samples based on **1** at concentrations of 100 and 400 mM.

concentrations, multiexponential decays are found, which represents a different situation from that of highly concentrated solutions[45] or PMMA solids.[16] The contribution from components with longer decay times increases with increasing chromophore concentration. The time decay traces for the concentrations 100 and 400 mM were analyzed using a two-component decay model, which resulted in lifetimes for the shorter components of approximately 240 and 310 ns, and for the longer 1700 and 3100 ns, respectively. Clearly, the shorter contribution is a nonresolved instant response from the detection system as the time-duration of the lamp pulse is shorter than 1 μs. Thus, residual fluorescence will show up as a short decay component. The longer decay times obtained in these sol–gel materials should be compared to decay values of the phosphorescence in THF and PMMA which are in the range of several hundreds of microseconds. Thus, the phosphorescence can be considerably quenched also in the glass matrix as shown here. However, as described in the following section, the microstructure of the glass matrix can be altered, allowing the presence of different concentrations of oxygen from the ambient atmosphere to quench the phosphorescent triplet state.

The results for glass samples of chromophore **2** and **3** showed the same general trends as those presented here for **1**, i.e., the emission spectra were dominated by fluorescence at low concentrations, below 1 mM, and phosphorescence, in the

dx.doi.org/10.1021/am2015537 | ACS Appl. Mater. Interfaces 2012, 4, 2369–2377

range 525−575 nm, when concentrations were increased to 50 mM and above. Also, similar trends were observed regarding the decay times.

As concluded from the PALS porosity measurements, different organosilane precursors resulted in very different matrix microstructures. Thus, AAPTES and PrAPTES showed undetectable porosity, whereas GLYMO and MTEOS resulted in considerably larger pores with average sizes 0.34 and 0.79 nm, respectively. The different matrix structures also had strong impact on the decays of the phosphorescence due to the amount and accessibility of dioxygen in the core of the glass materials. This has a direct effect on the phosphorescence of the final material and was readily demonstrated by irradiating the materials with UV/blue-light. Figure 9 shows the glowing

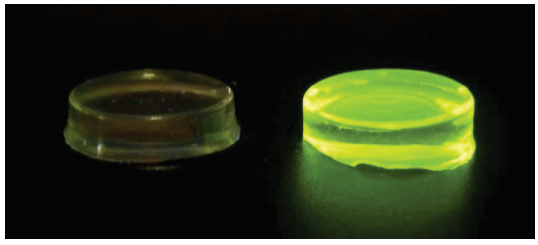

Figure 9. UV irradiation of **2**-MTEOS (left) and **2**-MTEOS-GLYMO (right) xerogels. Oxygen migrates into the pores of **2**-MTEOS and quenches the phosphorescence.

emission from the MTEOS and MTEOS-GLYMO-based glass materials loaded with chromophore **2**. While the former, having a microporous structure, starts to luminesce after several minutes of irradiation, the latter xerogel, with absence of larger pores, luminesces instantaneously. This can be correlated with the presence of oxygen in the glass material and the quenching of the phosphorescence of chromophore **2**. When the glass material has a microporous structure, as confirmed by PALS measurements, oxygen can diffuse into the core and interact with the dopant. This process is well-known for the Pt-acetylides as was originally shown using dendrimer functionalization.[34] After a few seconds the oxygen is consumed and decomposed into singlet oxygen and the material starts to luminesce.

Using the pulsed microsecond source the quenching process can be quantified in terms of the phosphorescence decay time as shown in Figure 10. AAPTES and PrAPTES had the smallest (negligible) sized pores and also showed a dramatically longer decay time than the porous matrices associated with GLYMO and MTEOS. The decay time for AAPTES and PrAPTES samples are indeed similar to values obtained for analogues of **2** (i.e., *trans*-bis(tributylphosphine)-di(4-ethynyl-1-(2-phenylethynyl)benzene)platinum in degassed THF solution[25] and an esterified derivative of **2** in PMMA glass[45]), with the phosphorescent decay times being up to hundreds of microseconds.

The evidence of the strong involvement of oxygen in quenching of the phosphorescence of the dopants was demonstrated by the observation of singlet oxygen emission at 1275 nm from the matrix/solute (data not shown), following excitation at 360−385 nm and triplet formation of the chromophores. For further details on singlet oxygen formation via quenching of the triplet state of other Pt-acetylides, see Glimsdal et al.[35]

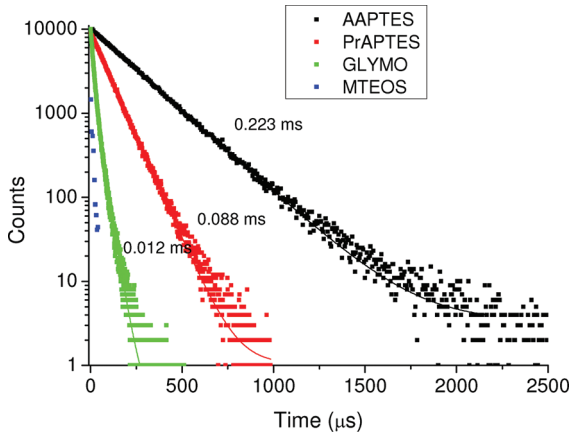

Figure 10. Excited state lifetime of chromophore **2** in different xerogel matrices. All decay traces were obtained for excitation in the range 360−385 nm and emission of the phosphorescence band at 520−530 nm.

NONLINEAR ABSORPTION OF LIGHT AND OPL OF THE HYBRID MATERIALS

The optical limiting performance of 50 (5% by weight), 100 (9% by weight) and 400 mM (30% by weight), MTEOS glasses doped with chromophore **1**, at 532 nm, using 5 ns laser pulses, is shown in Figure 11. As expected, the OPL effect increases

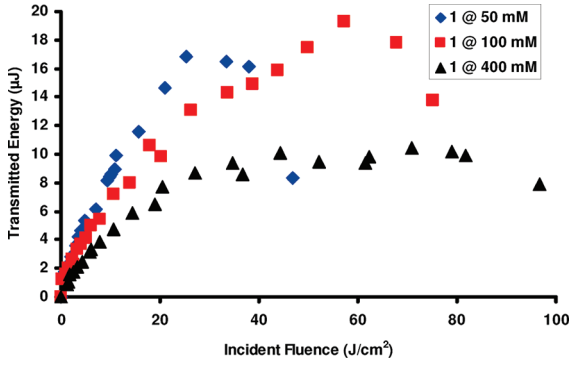

Figure 11. Incident fluence vs transmitted energy at 532 nm, using 5 ns laser pulses, for the 1 mm thick MTEOS glasses doped with chromophore **1** at concentrations of 50, 100, and 400 mM, with linear transmission of 88, 86, and 77%, respectively.

with increasing concentration of dopant. The sharp drop in the transmitted energy that appears in the figure at higher fluences, especially notable for the 50 and 100 mM samples, is due to laser induced damage of the materials. The laser damage threshold seems to increase with dopant mass %.

A comparison of the optical limiting response, at 532 nm, for silica glasses doped with 50 mM of chromophores **1**, **2**, and **3**, is shown in Figure 12. Previous solution studies have shown that an increase in conjugation length of the chromophore system has a positive impact on the nonlinear response,[23,25,46] which is also found for the MTEOS glasses. In addition, a drop in transmitted energy observed for **1** and **3** indicates that the material damage threshold increases with an increased chromophore conjugation length.

Earlier results on solutions of Pt-acetylides analogous to chromophore **2** have shown broadband nonlinear absorption at visible wavelengths.[23,27] OPL measurements at 500, 532, and 600 nm for the MTEOS glasses doped with 30 mass-% (400

dx.doi.org/10.1021/am2015537 | ACS Appl. Mater. Interfaces 2012, 4, 2369−2377

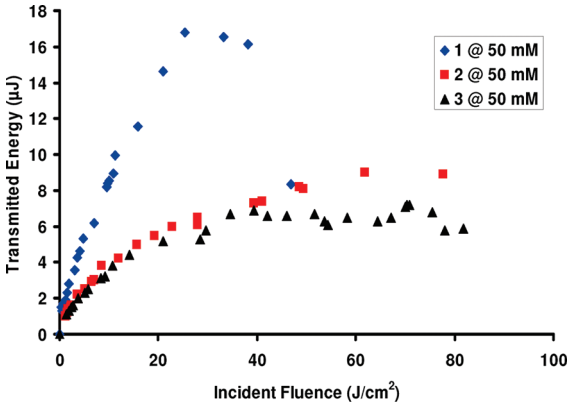

Figure 12. Incident fluence vs transmitted energy at 532 nm, 5 ns laser pulses, for 1 mm thick MTEOS glasses doped with 50 mM of chromophores **1**, **2**, and **3**, with linear transmission of 88, 87, and 85% respectively.

mM) of chromophore **2** (Figure 13) show clearly that this property is preserved in the new solid materials as presented here.

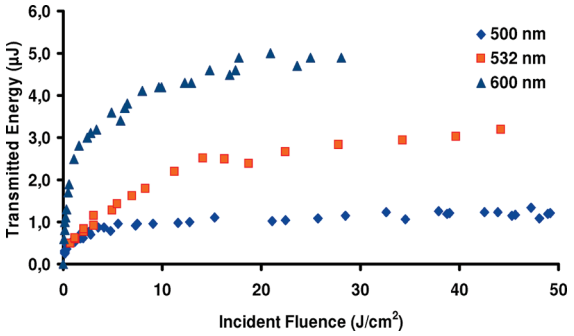

Figure 13. Incident fluence vs transmitted energy at 500, 532, and 600 nm, 5 ns laser pulses, for 1 mm thick MTEOS glasses doped with 30 mass % (400 mM) chromophore **2**. The linear transmission at the three wavelengths was 65, 73, and 78%, respectively.

SUMMARY AND CONCLUDING REMARKS

New hybrid organic–inorganic materials for optical applications based on sol–gel processing are prepared with a new approach. A unique feature of this approach is the control of the chemical condensation rates along with special additives during the densification step, allowing a load of molecular moieties for multiphoton absorption at extremely high concentrations. The solid materials can be polished and processed just as conventional sol–gel glasses. Moreover, the unique photophysical properties of the solutes are fully preserved from those in solution. The function is demonstrated by preparation of a series of sol–gel glasses doped with Pt-acetylide complexes at different concentrations. The MTEOS-based glasses show strong and broadband OPL response, and interestingly an increased damage threshold with increasing loading and with increased conjugation length of the chromophores. This study opens up a wide range of possible hybrid organic–inorganic glasses, even with poorly soluble chromophores, for a variety of advanced materials not only for pure photonics but also likely for applications in catalysis, biosensing or photovoltaics.

EXPERIMENTAL SECTION

A scheme of the synthesis of chromophores **1**–**3** and synthetic details are presented as Supporting Information.

General. Alkoxysilane precursors were purchased from ABCR. THF of nonstabilized HPLC grade and diethyl ether analysis grade stabilized with BHT from Carlo Erba were used. Milli-Q water (18 MΩ) was used for hydrolysis reactions.

Preparation of Materials. *Typical Procedure for the Preparation of the Sol for Hydrophobic Precursors (MTEOS, VTEOS).* MTEOS (100 mL) was hydrolyzed in acidic medium (H_2O with HCl, pH 3.8). The hydrolysis molar ratio water/precursor was 20. The mixture was stirred overnight at room temperature and evaporated to the initial volume of the precursor. This solution was placed at 2 °C for 1 week, allowing the decantation of a hydrophobic phase, rich of hydrolyzed and condensed MTEOS. This phase was dissolved in diethyl ether (150 mL) to remove residual water after phase separation. Then, diethyl ether was evaporated and replaced by THF so that the dried solid residue after evaporation of the solvents represents 30% in mass. This prepared sol can be stored at −24 °C and kept for several months.

Typical Procedure for the Preparation of the Sol for Partially Hydrophilic Precursors (GLYMO, AAPTES, BAPTES). Acidic water (HCl, pH 3.8) with a molar ratio $H_2O/Si = 20$ is added to a mixture of MTEOS (29.7 mL, 148 mmol) and GLYMO (3-Glycidoxypropyltriethoxysilane) (10.3 mL, 37 mmol) in a molar ratio of 4/1. The obtained solution is heated overnight at 100 °C. After cooling, the released alcohol and a part of water are removed under reduced pressure. The sol was dissolved in diethyl ether (80 mL) to remove residual water after phase separation. The turbid organic phase is dried on $MgSO_4$. Then, diethyl ether was evaporated and replaced by THF so that the dried solid residue after evaporation of the solvents represents 30% in mass.

Typical Procedure for the Preparation of a Hybrid Monolith. The chromophore is dissolved in the minimum of THF and added to 1 g of the sol under moderate heating (for example 45 °C) to increase the solubility. The mixture is stirred using an orbital stirrer for 5 min at room temperature and placed in a PTFE mold. APTES (45 µL) is quickly added to the mixture under stirring for 20 s (orbital stirrer) to induce fast condensation of the network at room temperature. The mold is closed. The gel is formed after a few minutes at room temperature. After gelation, the loaded mold is partially opened and put in a drier at 45 °C. The gel is slowly dried for 48 h at 45 °C and for another 24 h at 80 °C. The resulting xerogel glass materials with a doping up to 40% in mass (400 mM concentration) were prepared with chromophores **1** and **2**.

Cutting and Polishing. A Buehler Isomet 1000 Precision Saw was used to cut the transparent glass materials to the desired thickness. The polishing was performed with a Struers polishing equipment to the final 1 ± 0.05 mm.

^{29}Si NMR was performed on a Bruker DRX400 spectrometer. TMS in acetone-d6 in a separate capillary tube was used as reference. 128 scans were used during the experiments. The mono-, di- and tricondensed silanes had the chemical shifts −48, −57, and −66 ppm, respectively.

Specific surface areas were measured by the BET method at 77 K using N2 as adsorptive agent.

The positron annihilation lifetime spectrometer (PALS) used for the measurements was a standard fast coincidence system with a time resolution of 245 ps (fwhm). The measurements were performed at room temperature in air.

The nonlinear optical experiments were recorded at 500, 532 (SHG), and 600 nm using a frequency-doubled Nd:YAG laser equipped with a OPO delivering 5 ns pulses. Energies of the incident laser beam were attenuated by absorption filters in two filter wheels, which were combined to yield various optical densities. The beam was guided by mirrors into a spatial filter to remove imperfections in the beam's intensity profile. The beam then passed through a pellicle beam splitter, which diverted a small portion of the beam to a reference detector, used to monitor the incident energy. The transmitted beam was expanded in a simple telescope to about double its size, thus filling

dx.doi.org/10.1021/am2015537 | ACS Appl. Mater. Interfaces 2012, 4, 2369–2377

the entrance aperture and lens of the focusing system. The focusing lens, an achromatic doublet with focal length of 100 mm and f-number 5, was used to focus the beam to the center of the 1 mm thick glass materials. Single laser shots were used and the materials were moved vertically or horizontally before each shot to avoid damage caused by a beam focused at the same spot as previous beam. The transmitted energy was collimated by a second achromatic lens and passed through an aperture with 7 mm in diameter. The beam was then focused onto a signal detector. The signal and reference detectors were pyroelectric heads from Ophir, of type PD10-V1-SH (signal) and PE9 (reference).

The UV−vis transmission spectra were recorded using a CARY 5G UV−vis-NIR spectrophotometer. Excitation and emission spectra, along with time-resolved luminescence were recorded using an IBH 5000 submicrosecond xenon flashlamp as light source in conjunction with an IBH time-resolved spectrometer. For more details on the luminescence characterization, see refs 16, 28, 29, 34, 35, and 45.

■ ASSOCIATED CONTENT

Supporting Information

Details on the synthesis and characterizations of chromophores **1**−**3** (PDF). This material is available free of charge via the Internet at http://pubs.acs.org/.

■ AUTHOR INFORMATION

Corresponding Author

*E-mail: stephane.parola@univ-lyon1.fr.

Notes

The authors declare no competing financial interest.

■ ACKNOWLEDGMENTS

Support to B.E., C.L., C.B., J.Ö., and S.P. from the "Swedish Defence Research Agency" is gratefully acknowledged. M.L., D.C., and S.P. are grateful to the bilateral France-Norway Aurora project for travelling support. N.D. is on leave at IPN from INRNE, Academy of Sciences, Sofia, Bulgaria. Support to P.N. by the program PHC-RILA-25288XL and an agreement CNRS-Academy of Sciences of Bulgaria. N. Charvin is acknowledged for PALS measurements and L-G. Heimdal for cutting and polishing the glass materials.

■ REFERENCES

(1) Sanchez, C.; Lebeau, B.; Chaput, F.; Boilot, J.-P. *Adv. Mater.* **2003**, *15* (23), 1969.

(2) Boilot, J. P.; Biteau, J.; Brun, A.; Chaput, F.; Dantas de Morais, T.; Darracq, B.; Gacoin, T.; Lahlil, K.; Lehn, J. M.; Levy, Y.; Malier, L. *Mater. Res. Soc. Symp. Proc.* **1998**, *519*, 227.

(3) Canva, M.; Darracq, B.; Chaput, F.; Lahlil, K.; Bentivegna, F.; Brunel, M.; Falloss, M.; Georges, P.; Brun, A.; Boilot, J. P.; Levy, Y. *SPIE's 1998 International Symposium on Optics, Imaging and Instrumentation, Organic-Inorganic hybrid Materials for Photonics*; SPIE: Bellingham, WA, 1998; Vol. *3469*, p 164

(4) Judeinstein, P.; Sanchez, C. *J. Mater. Chem.* **1996**, *6*, 511.

(5) Desroches, C.; Lopes, C.; Kessler, V.; Parola, S. *Dalton Trans.* **2003**, 2085.

(6) Zieba, R.; Desroches, C.; Chaput, F.; Carlsson, M.; Eliasson, B.; Lopes, C.; Lindgren, M.; Parola, S. *Adv. Funct. Mater.* **2009**, *19*, 235.

(7) Riehl, D.; Chaput, F.; Levy, Y.; Boilot, J.-P.; Kajzar, F.; Chollet, P. A. *Chem. Phys. Lett.* **1995**, *245*, 36.

(8) Fallos, M.; Canva, M.; Georges, P.; Brun, A.; Chaput, F.; Boilot, J. P. *Appl. Opt.* **1997**, *36* (27), 6760.

(9) Biteau, J.; Chaput, F.; Boilot, J. P. *J. Phys. Chem.* **1996**, *100* (21), 9024.

(10) Darracq, B.; Canva, M.; Chaput, F.; Boilot, J. P.; Riehl, D.; Levy, Y.; Brun, A. *Appl. Phys. Lett.* **1997**, *70* (3), 1.

(11) Biteau, J.; Chaput, F.; Lahlil, K.; Boilot, J. P.; Tsivgoulis, G. M.; Lehn, J. M.; Darracq, B.; Marois, C.; Levy, Y. *Chem. Mater.* **1998**, *10* (7), 1945.

(12) Hench, L. L.; Orcel, F. G. U.S. patent 4 851 150, 1989.

(13) Hench, L. L. In *Science of Ceramics Chemical Processings*; Hench, L.L., Ulrich, D.R., Eds.; Wiley: New York, 1986; p 52.

(14) Hollins, R. C. *Curr. Opi. Solid State Mater. Sci.* **1999**, *4*, 189.

(15) Spangler, C. W. *J. Mater. Chem.* **1999**, *9*, 2013.

(16) Westlund, R.; Malmstrom, E.; Lopes, C.; Ohgren, J.; Rodgers, T.; Saito, Y.; Kawata, S.; Glimsdal, E.; Lindgren, M. *Adv. Funct. Mater.* **2008**, *18* (13), 1939.

(17) Brusatin, G.; Innocenzi, P.; Guglielmi, M.; Signorini, R.; Bozio, R. *Nonlinear Opt.* **2001**, *27*, 259.

(18) Innocenzi, P.; Brusatin, G. *Chem. Mater.* **2001**, *13*, 3126.

(19) Sanz, N.; Ibanez, A.; Morel, Y.; Baldeck, P. L. *Appl. Phys. Lett.* **2001**, *78* (17), 2569.

(20) Desroches, C.; Parola, S.; Cornu, D.; Miele, P.; Baldeck, P. L.; Lopes, C. *Mater. Res. Soc. Symp. Proc.* **2003**, *771*, 237.

(21) Örtenblad, M.; Parola, S.; Chaput, F.; Desroches, C.; Sigala, C.; Letoffe, J. M.; Miele, P.; Baldeck, P. L.; Eliasson, B.; Eriksson, A.; Lopes, C. *Mater. Res. Soc. Symp. Proc.* **2005**, *847*, 405.

(22) Parola, S.; Zieba, R.; Desroches, C.; Chaput, F.; Malmström, E.; Lindgren, M.; Eliasson, B.; Lopes, C. *Proc. SPIE* **2006**, 6401.

(23) Zhou, G.-J.; Won, W.-Y. *Chem. Soc. Rev.* **2011**, *40*, 2541.

(24) Cooper, T. M.; McLean, D. G.; Rogers, J. E. *Chem. Phys. Lett.* **2001**, *349*, 31.

(25) Rogers, J. E.; Cooper, T. M.; Fleitz, P. A.; Glass, D. J.; McLean, D. G. *J. Phys. Chem. A* **2002**, *106*, 10108.

(26) McKay, T. J.; Bolger, J. A.; Staromlynska, J.; Davy, J. R. *J. Chem. Phys.* **1998**, *108*, 5537.

(27) Staromlynska, J.; McKay, T. J.; Bolger, J. A.; Davy, J. R. *J. Opt. Soc. Am. B−Opt. Phys.* **1998**, *15*, 1731.

(28) Lind, P.; Bostrom, D.; Carlsson, M.; Eriksson, A.; Glimsdal, E.; Lindgren, M.; Eliasson, B. *J. Phys. Chem. A* **2007**, *111*, 1598.

(29) Glimsdal, E.; Carlsson, M.; Eliasson, B.; Minaev, B.; Lindgren, M. *J. Phys. Chem. A* **2007**, *111*, 244.

(30) Zhou, G.-J.; Wong, W.-Y.; Ye, C.; Lin, Z. *Adv. Funct. Mater.* **2007**, *17*, 963.

(31) Zhou, G.-J.; Wong, W.-Y.; Lin, Z.; Ye, C. *Angew. Chem., Int. Ed.* **2006**, *45*, 6189.

(32) Zhou, G.-J.; Wong, W.-Y.; Cui, D.; Ye, C. *Chem. Mater.* **2005**, *17*, 5209.

(33) Liao, C.; Shelton, A. H.; Kim, K.-Y.; Schanze, K. S. *ACS App. Mater. Interfaces* **2011**, *3*, 3225.

(34) Lindgren, M.; Minaev, B.; Glimsdal, E.; Vestberg, R.; Westlund, R.; Malmstrom, E. *J. Lumin.* **2007**, *124* (2), 302.

(35) Glimsdal, E.; Carlsson, M.; Kindahl, T.; Lindgren, M.; Lopes, C.; Eliasson, B. *J. Phys. Chem. A* **2010**, *114* (10), 3431.

(36) Sonogashira, K.; Yatake, T.; Tohda, Y.; Takahashi, S.; Hagihara, N. *J. Chem. Soc., Chem. Commun.* **1977**, 291.

(37) Chaput, F.; Parola, S.; Lopes, C.; Desroches, C.; Chateau, D. EU Patent EP 10305377.3-2111, 2010.

(38) Brunauer, S.; Emmett, P. H.; Teller, Ed. *J. Am. Chem. Soc.*, **1938**, *60* (2), 309.

(39) Brun, M.; Lallemand, A.; Quinson, J.-F.; Eyraud, C. *Thermochim. Acta* **1977**, *21*, 59.

(40) Jean, Y. C.; Mallon, P. E.; Schrader, D. M. *Principles and Applications of positron and Potronium Chemistry*; World Scientific Publishing Co. Pte. Ltd.: Singapore, 2003.

(41) Tao, S. J. *J. Chem. Phys.* **1972**, *56*, 5499.

(42) Eldrup, M.; Lightbody, D.; Sherwood, J. N. *Chem. Phys.* **1981**, *63*, 51.

(43) Gidley, D. W.; Frieze, W. E.; Dull, T. L.; Yee, A. F.; Ryan, E. T.; Ho, H.-M. *Phys. Rev. B* **1999**, *60*, R5157.

(44) Sudarshan, K.; Dutta, D.; Sharma, S. K.; Goswami, A.; Pujari, P. K. *J. Phys.: Condens. Matter.* **2007**, *19*, 386204.

(45) Glimsdal, E.; Norman, P.; Lindgren, M. *J. Phys. Chem. A* **2009**, *113* (42), 11242.

(46) Liu, R.; Li, Y.; Li, Y.; Zhu, H.; Sun, W. *J. Phys. Chem. A* **2010**, *114* (48), 12639.